Ceritinib overcomes proteasome inhibitor resistance in multiple myeloma by suppressing the protein folding response

Andrej Besse,[1,2] Marianne Kraus,[1] Tiberiu Totu,[3-5] Marija Buljan,[4,5] Antonius P.A. Janssen,[6] Mario van der Stelt,[6] Karin Matisikova,[2] Jana Veprkova,[2] Lenka Sedlarikova,[2] Tamara Jurinakova,[7] Marietta Truger,[8] Claudia Haferlach,[8] Max Mendez Lopez,[1] K. Martin Kortum,[9] Leo Rasche,[9] Christoph Driessen[1] and Lenka Besse[1,2]

[1]Laboratory of Experimental Oncology, Division Oncology and Hematology, HOCH Health Ostschweiz, Cantonal Hospital St. Gallen, St. Gallen, Switzerland; [2]Department of Biology, Faculty of Medicine, Masaryk University, Brno, Czech Republic; [3]Department of Health Sciences and Technology, Eidgenössische Technische Hochschule Zürich (ETH), Zurich, Switzerland; [4]Department Materials Meet Life, Swiss Federal Laboratories for Materials Science and Technology (Empa), St. Gallen, Switzerland; [5]Swiss Institute of Bioinformatics (SIB), Lausanne, Switzerland; [6]Department of Molecular Physiology, Leiden Institute of Chemistry, Leiden University & Oncode Institute, CC Leiden, the Netherlands; [7]Department of Pathophysiology, Faculty of Medicine, Masaryk University, Brno, Czech Republic; [8]MLL Munich Leukemia Laboratory, Munich, Germany and [9]Department of Internal Medicine II, University Hospital Würzburg, Würzburg, Germany

Correspondence: L. Besse
Lenka.besse@med.muni.cz
lenka.besse@h-och.ch

Received: September 23, 2025.
Accepted: December 5, 2025.
Early view: December 11, 2025.

https://doi.org/10.3324/haematol.2025.289245

Abstract

Proteasome inhibitor (PI) resistance remains a major therapeutic obstacle in the treatment of multiple myeloma (MM). MM cells demonstrate pronounced dependence on insulin and insulin-like growth factor-1 signaling via their cognate receptors, INSR and IGF-1R. In this study, we identify ceritinib, a clinically approved inhibitor of anaplastic lymphoma kinase, as a drug that can inhibit IGF-1R/INSR activity and downstream PI3K/AKT/mTORC1 signaling. Ceritinib can overcome PI-resistance in MM when used in combination with carfilzomib. This synergy was consistently observed across *in vitro* and *in vivo* models, and primary patient-derived MM cells. Mechanistically, MM cells exploit IGF-1R/INSR signaling to sustain expression of key molecular chaperones, including HSP70 and BiP, which are critical for maintaining proteostasis under conditions of high protein synthesis and turnover. Pharmacological inhibition of IGF-1R/INSR signaling by ceritinib abrogates this adaptive stress response, thereby preventing the upregulation of cytoprotective heat shock proteins upon proteasome inhibition. This disruption results in enhanced accumulation of protein aggregates, increased protein polyubiquitination, endoplasmic reticulum stress, and activation of apoptotic pathways. Collectively, our findings support the repurposing of ceritinib in combination with carfilzomib as a translationally relevant and safe strategy to circumvent PI resistance in MM, warranting further clinical investigation in the relapsed/refractory disease setting.

Introduction

Proteasome inhibitors (PI), including bortezomib and carfilzomib, are cornerstone therapies in the treatment of multiple myeloma (MM), effectively managing the disease in various clinical settings.[1] However, treatment with PI is not curative, and overcoming PI resistance remains a significant unmet medical need to improve patients' survival. PI are highly effective in MM due to the disease's unique dependency on the ubiquitin-proteasome system to maintain protein homeostasis, balancing high protein synthesis with proper degradation and recycling. To support protein homeostasis, MM cells adapt the size and function of the endoplasmic reticulum (ER) to fold proteins efficiently and prevent aggregation, relying on molecular chaperones, such as heat-shock proteins (HSP)70 and HSP90. In response to proteasome inhibition, MM cells further upregulate these chaperones, particularly HSP70, to stabilize proteins awaiting degradation and prevent their aggregation.[2,3] Accordingly, inhibition of HSP70 and HSP90 significantly sensitizes MM cells to PI.[4-6] However, despite their clinical promise,[4-6] HSP inhibitors have not translated into clinical

success, as trials to date have failed to produce Food and Drug Administration (FDA)-approved therapies due to these drugs' limited potency and narrow therapeutic window.[7]
In addition to the ubiquitin-proteasome system, insulin and insulin-like growth factor-1 (IGF-1) signaling play crucial roles in MM cell survival and resistance to PI. Both IGF-1 and insulin act as growth factors for MM, signaling through their respective receptors, IGF-1R and INSR,[8-10] which are highly homologous but mediate distinct cellular functions.[11] IGF-1R is involved in regulating genes that control cell proliferation, while INSR regulates genes related to metabolism and the glycolytic response to stimulation.[12] IGF-1R signaling has been linked to MM survival,[13] acquired resistance to bortezomib,[14] diminishing PI efficacy,[15] while INSR signaling remains less understood. Consequently, IGF-1R inhibition showed antitumor activity with a favorable *in vivo* therapeutic window.[13] Although inhibitors targeting IGF-1R and INSR have not been successful as single agents in clinical trials for MM, compounds that target other kinases, such as anaplastic lymphoma kinase (ALK), have shown off-target activity against IGF-1R/INSR. One such ALK inhibitor, ceritinib, which is FDA-approved for ALK-positive non-small cell lung cancer,[16] has shown the ability to reduce IGF-1R and INSR phosphorylation in preclinical cancer models[17-19] and could potentially provide a therapeutic approach for overcoming PI resistance in MM.
Recent studies have shown that ceritinib exhibits selective cytotoxicity in MM cell lines and patients' primary cells.[20] In this study, we show that ceritinib exhibits strong synergistic anti-MM effects with carfilzomib, both *in vitro* and *in vivo*. By inhibiting IGF-1R and INSR signaling, ceritinib disrupts the downstream PI3K/AKT/mTORC pathway and reduces the levels of HSP, leading to the accumulation of protein aggregates. This disruption impairs a pro-survival HSP response induced by carfilzomib, further triggering autophagy and apoptosis. These results highlight a promising and safe off-the-shelf combination therapy with the potential to overcome PI resistance in MM.

Methods

Cell lines

The MM cell lines, AMO-1, L363, RPMI-8226 and ARH-77, were purchased from the American Type Cell Collection (ATCC) or the German Collection of Microorganisms and Cell Cultures (DSMZ). Cell lines adapted to bortezomib (AMO-BTZ, L363-BTZ, RPMI-BTZ, ARH-BTZ) or carfilzomib (AMO-CFZ, L363-CFZ, RPMI-CFZ, ARH-CFZ) were grown in the presence of 90 nM of the respective inhibitors as previously described.[21]

Patients' samples

Samples from patients with MM or plasma cell leukemia (PCL) and peripheral blood mononuclear cells from healthy volunteers were obtained at Cantonal Hospital St. Gallen, Switzerland. All samples were obtained during routine diagnostic procedures after approval by an independent cantonal ethical committee (EKSG 09/057). Written informed consent was obtained in accordance with the Declaration of Helsinki guidelines. The patients' baseline characteristics are shown in *Online Supplementary Table S1*. PCL samples were obtained from peripheral blood, whereas MM samples were purified from bone marrow aspirates; the $CD138^+$ plasma cells were enriched by $CD138^+$ selection using an EasySep Human Whole Blood and Bone Marrow CD138 Positive Selection Kit (StemCell Technologies, Vancouver, Canada).

In vivo experiments

Age-matched (8-10 weeks old) male and female NSG (NOD.CB17-Prkdc^{scid}/NCrCrl) mice (Charles River, Germany) were used in the experiment, in accordance with the protocol approved by the Committee for Animal Experiments (Czech Republic); application number MSMT-16038/2024-3. One week after the intrafemoral injection of AMO-BTZ cells (50,000 cells) equipped with TdTomato and Luciferin (RRID:Addgene_72486, a kind gift from Kazuhiro Oka), treatment with vehicle (captisol, twice a week, intravenous), carfilzomib (4 mg/kg, twice a week, intravenous), ceritinib (25 mg/kg, daily, intraperitoneal), or a drug combination was initiated for 2 weeks. The animals were randomly assigned to the treatment groups. Myeloma growth was monitored twice a week with luciferin (150 mg/kg, subcutaneous) (BioVision/Abcam; Waltham, MA, USA) using a LagoX imaging system (Spectral Instruments Imaging, Tucson, AZ, USA) during the entire course of the experiment. Blood glucose and hemoglobin levels were determined from a drop of blood once weekly using an ACCUGENCE PLUS Multi-Monitoring system (PM800).

Genome-wide CRISPR/Cas9 screening

A genome-wide screen was performed in the AMO-1 cell line using the Human CRISPR Knockout Pooled Library (Brunello, RRID:Addgene_73179, a kind gift from David Root and John Doench), following established protocols.[22] A screen with increasing doses of ceritinib (starting from 1 μM to 2.5 μM) was performed over 18 days (representing 10 doubling times) to identify genes whose loss sensitized the cells to a low concentration of ceritinib or allowed cell survival in the presence of higher concentrations of ceritinib, decreasing viability to 50%. Screening data were analyzed using MaGeCK-VISPR software.[23] False discovery rate (FDR) values <0.01 were considered statistically significant.

PamGene kinase screening

A kinase screening to identify kinase inhibition following 30 minutes of treatment with ceritinib in AMO-1 cells was performed using PamChip® microarrays (PamGene, the Netherlands). A detailed description is provided in the *Online Supplementary Material*.

Analysis of the Multiple Myeloma Research Foundation CoMMpass dataset

Transcriptomics data were downloaded from the CoMMpass℠ study, IA-18 and included 544 MM samples (*www.themmrf.org*). These data were generated as part of the Multiple Myeloma Research Foundation personalized medicine initiatives (*https://research.themmrf.org*).

More information can be found in the *Online Supplementary Material*.

Results

ALK inhibitors in combination with carfilzomib are cytotoxic to multiple myeloma cells *in vitro* and *in vivo*

To evaluate which ALK inhibitors exert cytotoxic effects in MM cells *in vitro*, we tested a panel of FDA-approved or clinically investigated ALK inhibitors (crizotinib, ceritinib, alectinib, brigatinib, ensartinib, lorlatinib, entrectinib) in two PI-naïve MM cell lines (AMO-1 and L363) and their bortezomib-resistant counterparts (AMO-BTZ and L363-BTZ). Among these, ceritinib, brigatinib, and entrectinib showed the greatest efficacy. In contrast, alectinib and lorlatinib showed minimal cytotoxic effects (Figure 1A, *Online Supplementary Table S2*).

We selected ceritinib for further studies and confirmed strong synergy of ceritinib and carfilzomib in several PI-resistance models (Table 1, *Online Supplementary Figures S1-S4*). To evaluate clinical relevance, we tested the combination in primary cells isolated from MM and PCL patients who had relapsed after or progressed on PI-containing therapies. The combination demonstrated a synergistic cytotoxic effect in all patients' samples tested (Figure 1B). The mean half maximal inhibitory concentration (IC_{50}) of

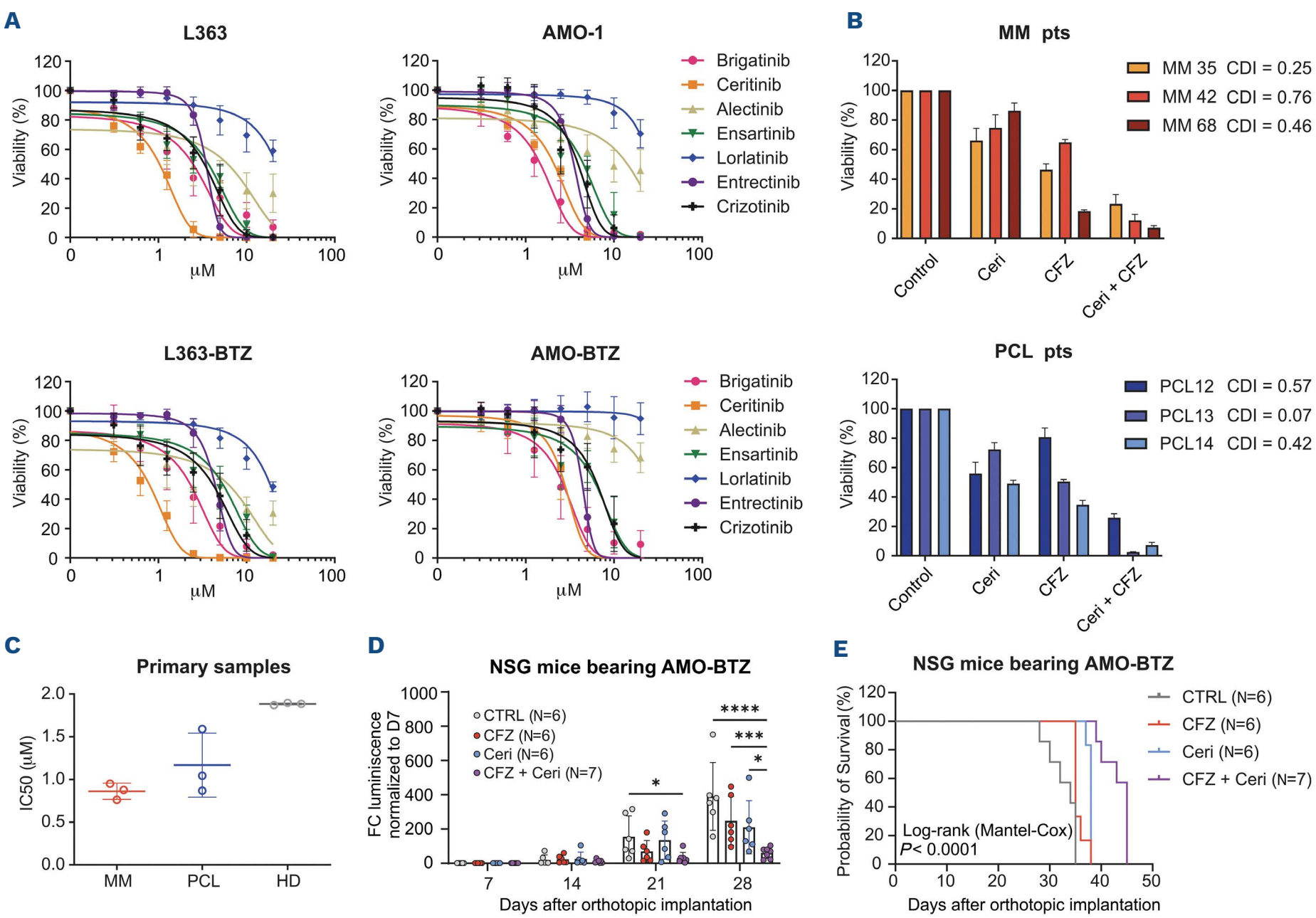

Figure 1. The combination of ceritinib and carfilzomib exhibits strong synergistic activity both *in vitro* and *in vivo*. (A) Dose–response curves of seven clinically available ALK inhibitors in proteasome inhibitor (PI)-naïve multiple myeloma (MM) cell lines (L363 and AMO-1) and their bortezomib-adapted counterparts (L363-BTZ and AMO-BTZ). The data represent the mean ± standard deviation (SD) from at least three independent biological replicates. (B) Cytotoxicity of the ceritinib and carfilzomib combination in primary samples from MM patients (red scale) and plasma cell leukemia (PCL) patients (blue scale). A coefficient of drug interaction was calculated for each patient. The data represent the

Continued on following page.

mean ± SD from technical quadruplicates. (C) Half maximal inhibitory concentration (IC_{50}) values for ceritinib in primary samples from MM and PCL patients, as well as in peripheral blood mononuclear cells from healthy donors. The data represent ranges from three individual samples per cohort. (D) *In vivo* imaging of luminescence intensity from orthotopically implanted AMO-BTZ cells, shown as fold change normalized to day 7 (treatment initiation). The number of animals per group is indicated in the treatment conditions. The data represent the mean ± SD for each treatment cohort. Statistical significance was assessed by two-way analysis of variance with the Tukey *post-hoc* test: ****P<0.0001, ***P<0.001, **P<0.01, *P<0.05. (E) Kaplan-Meier curves illustrating survival of mice with orthotopically implanted AMO-BTZ cells and treated with the respective drugs and their combination. The number of animals per group is indicated in the treatment conditions. Statistical analysis was performed using the log-rank (Mantel-Cox) test. pts: patients; CDI: coefficient of drug interaction; ceri: ceritinib; CFZ: carfilzomib; HD: healthy donors; PBMC: peripheral blood mononuclear cells.

ceritinib in MM patients' samples was 1.21 μM, while no cytotoxicity was observed in peripheral blood mononuclear cells from three healthy donors at doses up to 12.8 μM (Figure 1C), suggesting a favorable therapeutic window. Finally, we tested the combination *in vivo* using NSG mice injected intrafemorally with luciferase-expressing AMO-BTZ cells, allowing real-time tumor monitoring within the bone marrow niche. Carfilzomib alone had minimal therapeutic effects, consistent with *in vitro* cross-resistance of AMO-BTZ cells to carfilzomib.[24] However, ceritinib significantly reduced tumor burden as a monotherapy, and its combination with carfilzomib markedly suppressed tumor growth, especially at later time points (Figure 1D). This translated into prolonged survival in treated animals (Figure 1E). Drugs as monotherapy and in combination were safe and did not significantly affect the weight, glucose or hemoglobin level of the mice during the course of the treatment (*Online Supplementary Figure S5A-C*). Collectively, these data demonstrate that the combination of ceritinib and carfilzomib effectively overcomes PI resistance in MM across *in vitro*, *ex vivo* and *in vivo* models, even in the context of bone marrow stromal support.

Table 1. Coefficients of drug interaction for ceritinib in combination with either bortezomib or carfilzomib, as determined from viability assays (*Online Supplementary Tables S1–S4*) in a panel of proteasome inhibitor-naïve, bortezomib-adapted, and carfilzomib-adapted cell lines.

Cell line	Ceritinib combination, CDI	
	Bortezomib	Carfilzomib
AMO-1	0.96	0.14
AMO-BTZ	0.79	0.18
AMO-CFZ	0.24	0.07
L363	0.86	0.55
L363-BTZ	0.6	0.43
L363-CFZ	0.07	0.23
ARH-77	0.97	0.77
ARH-BTZ	0.55	0.16
ARH-CFZ	0.07	0.08
RPMI-8226	0.97	0.13
RPMI-BTZ	0.52	0.32
RPMI-CFZ	0.39	0.2

CDI: coefficient of drug interaction.

Ceritinib targets the IGF-1R/INSR pathway to reverse proteasome inhibitor resistance in multiple myeloma

To identify kinases that are inhibited by ALK inhibitors in MM, we interrogated the ChEMBL database for shared off-target receptor tyrosine kinases among the ALK inhibitors that were effective in MM at low concentrations (ceritinib, brigatinib, entrectinib), but not among those that were ineffective (alectinib, lorlatinib). This analysis revealed that alectinib and lorlatinib are highly selective for ALK, whereas ceritinib, brigatinib, and entrectinib also target FLT3, INSR, and IGF-1R at low nanomolar concentrations (*Online Supplementary Table S3)*.

To validate that ceritinib's efficacy in MM is primarily mediated via IGF-1R/INSR inhibition, we conducted a kinase profiling assay in AMO-1 cells. The results demonstrated selective inhibition of INSR and IGF-1R following treatment with ceritinib (Figure 2A), alongside other non-receptor tyrosine kinases physiologically involved in B-cell receptor (BTK, BLK), T-cell receptor (LCK, ZAP70) and other types of signaling (FES, SRC), while no inhibition of FLT3 was observed. To investigate the relevance of these targets in MM, we assessed their expression in MM patients' samples from the CoMMpass dataset. The results showed consistently high expression of INSR in the majority of patients. IGF-1R expression was present, but low in almost all patients. ALK, FLT3, BLK, LCK, ZAP70, and FES were mostly negligible or undetectable. In addition, expression of BTK and SRC was relatively high in the majority of patients (Figure 2B). Expression data from PI-naïve and PI-resistant MM cell lines used in this study corroborated these findings (*Online Supplementary Figure S6*). Additionally, data from the Cancer Dependency Map (DepMap, *www.depmap.org*) indicated that plasma cell myeloma exhibits increased dependency on INSR and IGF-1R (*Online Supplementary Figure S7, Online Supplementary Table S4*) for survival, in contrast to BTK and SRC, further supporting its functional relevance in MM.

We next tested whether direct inhibition of the IGF-1R/INSR pathway with two small-molecule inhibitors of IGF-1R/INSR (BMS-536924 and NVP-AEW541) could reproduce the synergy observed between ceritinib and carfilzomib in both PI-naïve (AMO-1, L363) and PI-resistant (AMO-BTZ, L363-BTZ) cells. Application of either of the small-mole-

cule inhibitors in combination with carfilzomib exhibited strong synergistic cytotoxicity, particularly in PI-resistant cells (Figure 2C, D). Notably, combining BMS-536924 or NVP-AEW541 with ceritinib did not result in additional synergy, suggesting that these agents converge on the same signaling pathway (*Online Supplementary Figure S8*).

In summary, these findings demonstrate that ceritinib modulates PI resistance in MM by targeting the IGF-1R/INSR axis, and that this pathway plays a critical role in mediating resistance to proteasome inhibition.

The PI3K/Akt/mTORC1 pathway is a key mediator of ceritinib-induced cytotoxicity in multiple myeloma

To identify key genes and signaling pathways mediating the cytotoxic effects of ceritinib in MM, we conducted a CRISPR/Cas9 genome-wide screen in AMO-1 cells. The screen identified 17 candidate resistance genes (FDR <0.01; $\log_2$ fold change >1) and two candidate sensitivity genes (FDR <0.01; $\log_2$ fold change < –1) (Figure 3A; *Online Supplementary Table S5*). Among the resistance hits, *FOXO1, NPRL2, NPRL3, DDIT4, TSC2*, and *TSC3* (all known negative

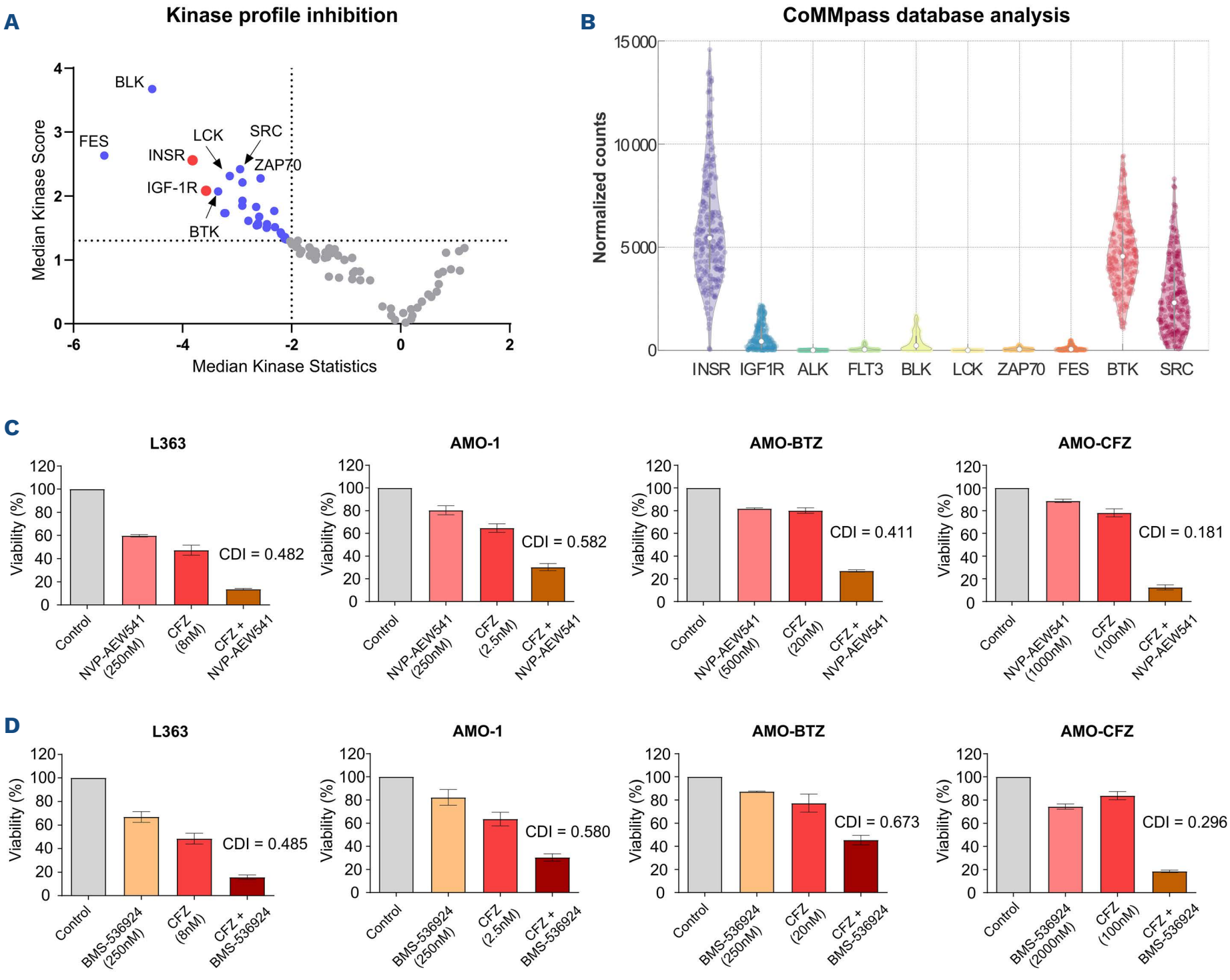

Figure 2. Ceritinib enhances carfilzomib efficacy by targeting highly expressed INSR/IGF-1R in multiple myeloma. (A) Volcano plot depicting the kinase inhibition profile in AMO-1 cells 30 minutes after treatment with 4 μM ceritinib. Insulin-like growth factor 1 receptor (IGF-1R) and insulin receptor (INSR) are highlighted in red. (B) Violin plot illustrating the expression of the off-target kinases identified by ceritinib in a cohort of 590 newly diagnosed multiple myeloma (MM) patients, based on the Multiple Myeloma Research Foundation CoMMpass dataset. The data represent normalized transcript counts. (C) Cytotoxic effects of carfilzomib (CFZ) and the IGF-1R/INSR small molecule inhibitor NVP-AEW541 in proteasome inhibitor (PI)-naïve (AMO-1, L363) and PI-adapted (AMO-BTZ, AMO-CFZ) cell lines. The data represent the mean ± standard deviation (SD) from three independent biological replicates. Coefficients of drug interaction (CDI) for combination treatment are presented. (D) Cytotoxic effects of CFZ and the IGF-1R/INSR inhibitor BMS-536924 in PI-naïve (AMO-1, L363) and PI-adapted (AMO-BTZ, AMO-CFZ) cell lines. The data represent the mean ± SD from three independent biological replicates. CDI for combination treatment are presented.

regulators of mTORC1 signaling) were prominently enriched. These genes were also recognized as co-dependent in prior large-scale screens.[25] As FOXO transcription factors and mTORC1 represent key downstream targets of the PI3K/Akt pathway, this suggests that ceritinib may exert its anti-myeloma effects through suppression of this axis. To independently validate our screen and assess reproducibility in additional cell lines, we pharmacologically

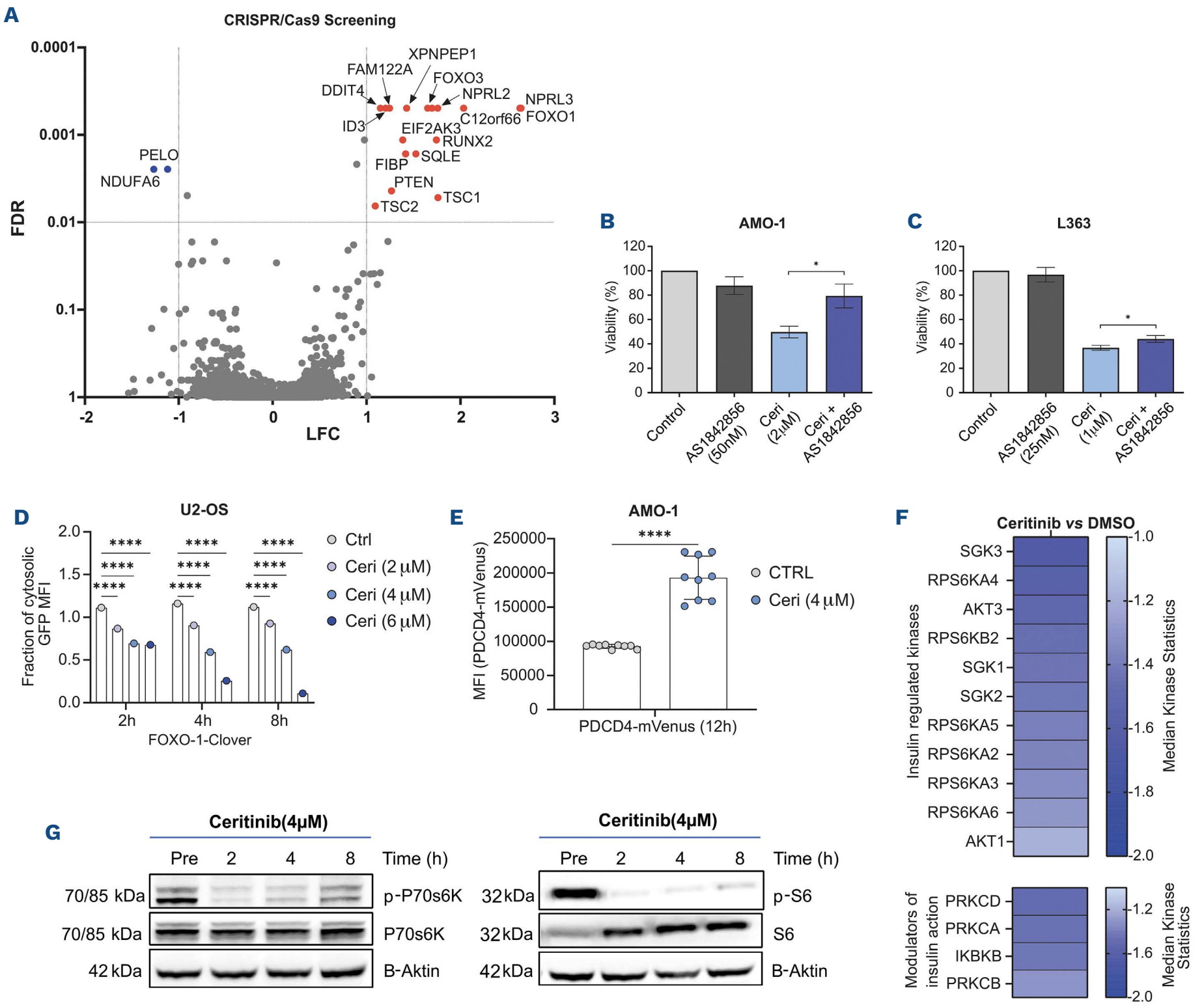

Figure 3. Ceritinib inhibits downstream PI3K/Akt/mTORC1 signaling in multiple myeloma cells via inhibition of IGF-1R/INSR. (A) Volcano plot showing sensitivity (blue) and resistance (red) genes to ceritinib, identified through a genome-wide CRISPR/Cas9 screen performed in AMO-1 cells. (B, C) Validation of CRISPR screen hits using the FOXO1 small-molecule inhibitor AS1842856 in AMO-1 (B) and L363 (C) multiple myeloma (MM) cell lines, either as monotherapy or in combination with ceritinib. The data represent the mean ± standard deviation (SD) from three independent biological replicates. Statistical significance was determined using two-way analysis of variance (ANOVA) with a Tukey *post-hoc* test; *P<0.05. (D) Quantification of FOXO1-clover nucleolar translocation in the U2-OS model cell line expressing a nucleolar mCherry reporter. The fraction of cytosolic GFP-only signal was measured at 2, 4 and 6 hours following treatment with the indicated doses of ceritinib. The data represent the mean ± SD from four replicates. Statistical significance was assessed by two-way ANOVA with a Tukey *post-hoc* test; ****P<0.0001. (E) Quantification of PDCD4-mVenus fluorescence intensity in AMO-1 cells 12 hours after treatment with 4 μM ceritinib. The data represent the mean ± SD of three independent experiments, each performed in triplicate. Statistical significance was determined by an unpaired *t* test; ****P<0.0001. (F) STK inhibited by ceritinib in AMO-1 cells following 8 hours of treatment with 4 μM ceritinib, ranked by median kinase score as calculated by PamGene analysis and grouped according to insulin-related processes defined by KEGG pathway annotations. (G) Western blot image showing phosphorylation levels of ribosomal p70 S6 kinase and ribosomal S6 protein after treatment with 4 μM ceritinib. KEGG: Kyoto Encyclopedia of Genes and Genomes; FDR: false discovery rate; LFC: log fold change; GFP: green fluorescence protein; MFI: mean fluorescence intensity; Ctrl/CTRL: control; Ceri: ceritinib; DMSO: dimethylsulfoxide.

inhibited FOXO1 using the selective inhibitor AS1842856. Combination treatment with AS1842856 significantly attenuated ceritinib-induced cytotoxicity in both AMO-1 and L363 cells (Figure 3B, C), confirming FOXO1 as a functional mediator of ceritinib response.

We next used functional reporter assays to monitor ceritinib's effects on PI3K/Akt signaling. In the first model, U2-OS cells expressing FOXO1-Clover and a nucleolar mCherry reporter were used to visualize FOXO1 nuclear translocation, a hallmark of PI3K/Akt inhibition. Treatment with ceritinib caused rapid translocation of green fluorescence protein (GFP) from the cytosol to the nucleus, consistent with pathway suppression (Figure 3D). In the second model, we assessed mTORC1 activity in AMO-1 cells using a target of mTOR signaling indicator (TOSI) construct, in which PDCD4 is tagged with mVenus. PDCD4 is rapidly degraded upon mTORC1 activation, thus its stabilization reflects mTORC1 inhibition. Following 12 hours of exposure to ceritinib, PDCD4 levels were significantly elevated in AMO-1 cells (Figure 3E), further supporting the suppression of mTORC1 activity. Additionally, kinome profiling in AMO-1 cells revealed that ceritinib inhibited multiple intracellular serine/threonine kinases regulated by insulin signaling, including several ribosomal S6 kinases, as annotated in the Kyoto Encyclopedia of Genes and Genomes (KEGG) pathway database (Figure 3F). Consistently, immunoblotting demonstrated reduced phosphorylation of both p70 S6 kinase and ribosomal protein S6, key downstream components of the mTORC1-driven translation machinery (Figure 3G, *Online Supplementary Figure S9*).

Collectively, these results indicate that ceritinib exerts its anti-MM activity primarily through suppression of the PI3K/Akt/mTORC1 pathway, leading to FOXO1 activation, inhibition of protein synthesis, and restoration of tumor suppressive signaling.

Ceritinib impairs the heat shock response and enhances endoplasmic reticulum stress induction by carfilzomib, shifting the balance toward apoptosis

To elucidate the molecular mechanism underlying the synergy between ceritinib and carfilzomib we performed transcriptomic profiling of differently expressed genes in AMO-1 cells 8 hours after the single and combinatorial treatments (*Online Supplementary Table S6*). Gene set enrichment analysis of ceritinib-induced expression changes, as well as gene ontology classification based on biological processes, revealed that ceritinib monotherapy suppressed pathways associated with DNA replication, ribonucleoprotein complex processing, and protein folding (Figure 4A, *Online Supplementary Figure S10A, Online Supplementary Table S7*). Notably, individual genes from the significantly enriched process of protein folding are HSP involved in processing of proteins in the ER, and response to unfolded/misfolded proteins (Figure 4A, B), as well as proteasome-encoding genes (Figure 4C). This is consistent with previous findings that insulin/IGF-1 signaling induces HSP expression.[26] In parallel, gene set enrichment analysis followed by network analysis and transcription factor target analysis (based on WebGestalt) identified E2F as a central transcription regulator of the ceritinib-repressed gene set (*Online Supplementary Figure S10B*), with individual genes reflecting impaired cell cycle progression (*Online Supplementary Figure S10C*). Genes induced by ceritinib were enriched for targets of the FOXO1 transcription factor (*Online Supplementary Figure S10D, E*), consistent with inhibition of PI3K/Akt signaling.

Carfilzomib monotherapy, as expected, induced the expression of genes associated with protein folding (HSP proteins), ER stress and the proteasome (Figure 4A-C, *Online Supplementary Figure S10F, Online Supplementary Tables S6* and *S7*), consistent with previous reports.[3] At the same time, it suppressed cell cycle progression and DNA replication-associated genes (*Online Supplementary Table S8*). The combination of ceritinib and carfilzomib enhanced the ER stress response as evidenced by the induction of genes related to the biological processes, topologically incorrect proteins, ER stress and autophagy (Figure 4B, *Online Supplementary Figure S10G, H*). Interestingly, despite stronger induction of ER stress, the response to protein misfolding and associated proteasome assembly appeared attenuated with the combination therapy compared to carfilzomib monotherapy (Figure 4A, C), suggesting that ceritinib co-treatment impairs the critical pro-survival response typically elicited by proteasome inhibition.[3]

Consistently, genes regulated by FOXO1, robustly induced by ceritinib alone, were also found to be elevated following combination treatment (*Online Supplementary Table S9, Online Supplementary Figure S10E*), indicating sustained Akt signaling suppression. Moreover, the combination led to a pronounced downregulation of genes involved in DNA replication and cell cycle progression (Figure 4F, *Online Supplementary Table S9*), with enrichment for E2F-target repression (*Online Supplementary Figure S10C*).

To explore the metabolic changes induced by single and combination treatments, we conducted an untargeted metabolomic analysis of metabolites following 8 hours of treatment with each drug alone and in combination (*Online Supplementary Table S10*). Ceritinib and the combination treatment reduced the levels of metabolites associated with glycolysis and the 'Warburg effect', consistent with INSR inhibition.[27] Consequently, the combination treatment led to a reduction of pyrimidines and accumulation of purine degradation products (guanosine, guanine, hypoxanthine, and xanthine) (Figure 4D), suggesting a disruption in nucleotide recycling for DNA and RNA synthesis, consistent with cell cycle arrest and imbalance in nucleotide synthesis.

At the protein level, immunoblot analysis confirmed key changes in the protein folding response, manifested as reductions in HSP70 and HSPA5 (GRP78, BiP) following ceritinib treatment, both as monotherapy and in combination with

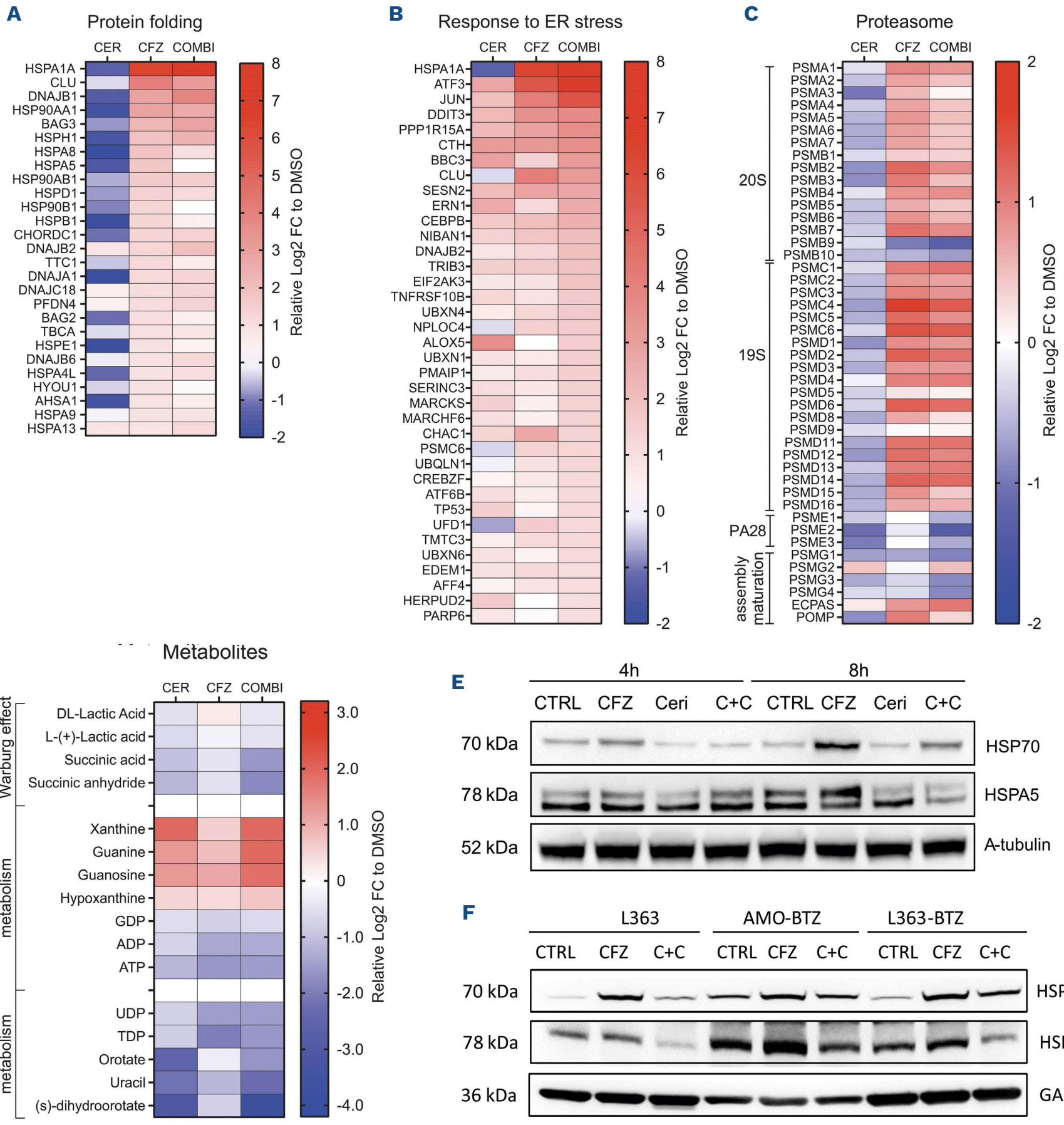

Figure 4. Ceritinib diminishes the endoplasmic reticulum stress and protein folding response, a key pro-survival pathway following proteasome inhibition. (A) Heatmap of leading-edge genes deregulated in AMO-1 cells 8 hours after treatment with ceritinib, carfilzomib, or their combination, clustered according to the 'Protein folding' Gene Ontology (GO) biological processes (BP) term. Depicted are genes with $\log_2$FC >0.8 (adjusted *P*<0.05) for carfilzomib (CFZ) and $\log_2$FC <0.8 for ceritinib. (B) Heatmap of leading-edge genes upregulated in AMO-1 cells 8 hours after treatment with ceritinib, carfilzomib, or their combination, clustered according to the 'Response to endoplasmic reticulum stress' GO BP term. Depicted are genes with $\log_2$FC >0.8 for CFZ + ceritinib treatment (adjusted *P*<0.05). (C) Heatmap of leading-edge genes upregulated in AMO-1 cells 8 hours after treatment with 4 μM ceritinib, 5 nM carfilzomib, and their combination, clustered according to the 'Proteasome' GO BP term. The data were normalized to untreated control samples and represent $\log_2$ FC values. (D) Heatmap of significantly deregulated metabolites involved in glucose (Warburg effect) and purine/pyrimidine metabolism following 8 hours of treatment with 4 μM ceritinib, 5 nM carfilzomib and their combination. The data were normalized to untreated control samples at the same timepoint and represent $\log_2$ FC values (adjusted *P*<0.05). (E) Western blot analysis showing levels of heat shock proteins HSP70 and HSPA5 (GRP78, BiP) at 4 and 8 hours following treatment with 4 μM ceritinib, 5 nM carfilzomib, or their combination (C+C) in AMO-1 cells. (F) Western blot analysis showing levels of heat shock proteins HSP70 and HSPA5 (GRP78, BiP) in L363, AMO-BTZ and L363-BTZ cell lines 8 hours after treatment with 5 nM carfilzomib, or a combination of carfilzomib with 4 μM ceritinib (C+C). CER: ceritinib; CFZ: carfilzomib; COMBI: combination of ceritinib and carfilzomib; ER: endoplasmic reticulum; FC: fold change; DMSO: dimethylsulfoxide; CTRL: control.

carfilzomib, compared to their levels in either untreated or carfilzomib-treated PI-naïve and PI-resistant cells (Figure 4E, F, *Online Supplementary Figure S11A, B*). These data support the findings observed at the transcriptome level and highlight a mechanistic shift from a cytoprotective to pro-apoptotic ER stress response during combination treatment.

Ceritinib and carfilzomib co-treatment disrupts pro-survival protein folding, triggering endoplasmic reticulum stress, polyubiquitin accumulation, autophagy, and apoptosis

Next, we investigated how ceritinib and carfilzomib co-treatment affects protein homeostasis. Using activity-based probes, we first confirmed that carfilzomib inhibits proteasome β5 subunit activity and partially inhibits β2 and β1 subunits, leading to the accumulation of polyubiquitinated proteins (K48-Ub proteins) (Figure 5A). While ceritinib alone did not have a direct effect on proteasome activity, its combination with carfilzomib led to significant poly-Ub accumulation (Figure 5A, *Online Supplementary Figure S12*). This finding was corroborated using the Ub-G76V-GFP reporter system, in which ceritinib and carfilzomib led to significantly greater accumulation of Ub-G76V-GFP compared to carfilzomib alone, whereas ceritinib monotherapy had no significant impact (Figure 5B).

We next evaluated the formation of toxic intracellular protein aggregates. Carfilzomib alone did not substantially induce aggregation, likely due to a compensatory heat-shock response that stabilizes unfolded/misfolded proteins.[3] In contrast, ceritinib monotherapy triggered the formation of aggresomes, and this effect was markedly enhanced by co-treatment with carfilzomib in both PI-naïve and BTZ-resistant MM cells, suggesting a mechanism for overcoming PI resistance (Figure 5C).

To assess how this accumulation of misfolded and ubiquitinated proteins impacts the unfolded protein response, we used AMO-1 cells equipped with fluorescent XBP1 splicing (XBP1s) reporter. As expected, carfilzomib strongly induced XBP1s after 8 hours, consistent with increased proteotoxic stress. Ceritinib alone caused only modest XBP1s induction, but combination treatment significantly enhanced XBP1s activation (Figure 5D).

We further evaluated the induction of autophagy using AMO-1 cells equipped with a tandem GFP/RFP-LC3 reporter. Ceritinib, but not carfilzomib, significantly induced autophagy within 8 hours (Figure 5E), consistent with mTORC1 inhibition. Notably, the ceritinib-induced autophagic flux at lower drug concentration (2 μM) was further enhanced by carfilzomib, in line with transcriptomic data.

To link these observations mechanistically to mTORC1 inhibition in MM cells, we used AMO-1 cells equipped with PDCD4-mVenus as a reporter. Although carfilzomib alone also led to PDCD4 accumulation – likely due to blocked proteasomal degradation – the combination significantly amplified this effect, indicating cooperative suppression of mTORC1-mediated PDCD4 turnover (Figure 5F). Subsequently, the ceritinib and carfilzomib combination significantly promoted both early and late apoptosis 24 hours after treatment (Figure 5G). Together, these findings demonstrate that co-inhibition of the proteasome and PI3K/Akt/mTORC1 signaling in MM disrupts protein quality control by impairing chaperone-mediated folding, enhancing polyubiquitinated protein accumulation, and triggering autophagy.

Candidate ceritinib-resistance genes are associated with poor prognosis in multiple myeloma

We next evaluated the prognostic significance of genes involved in ceritinib's mechanism of action in newly diagnosed MM patients from the CoMMpass dataset. Neither IGF-1R nor INSR showed a significant prognostic impact in this cohort (*Online Supplementary Figure S13A, B*). However, the highest-ranking ceritinib resistance candidates from the CRISPR screening, NPRL3 and FOXO-1, were significantly associated with poorer survival outcomes. High NPRL3 expression was associated with worse progression-free survival and overall survival (Figure 6A, *Online Supplementary Figure S13C*), while low FOXO-1 expression was only linked to shorter progression-free survival (Figure 6B, *Online Supplementary Figure S13D*), but not to OS, as previously described.[28]

Additionally, high expression of DDIT4, a negative regulator of mTORC1 signaling, was significantly associated with worse progression-free and overall survival (Figure 6C, *Online Supplementary Figure S13E*), while a low level of PDCD4, a marker of mTORC1 activity,[29,30] was associated with worse overall survival (*Online Supplementary Figure S13F*) in the CoMMpass dataset. We also compared patients from the CoMMpass dataset with relapsed/refractory MM patients from University Hospital Wurzburg. IGF-1R and INSR expression was significantly elevated in the relapsed/refractory cohort of patients (Figure 6D).

Overall, these findings provide proof-of-concept that increased PI3K/Akt/mTORC1 activity may be associated with poorer outcomes and suggest that, in these patients and those with advanced-stage MM, combining ceritinib with carfilzomib could offer a promising therapeutic approach.

Discussion

Although the IGF-1/insulin shared pathway that starts with two different receptors contributes to MM pathogenesis and resistance to standard therapies, targeting this system has shown limited clinical success, largely due to its complexity.[31] Clinical trials of IGF-1R/INSR inhibitors have yielded disappointing results due to poor efficacy, underscoring the need for novel approaches and combination strategies. Through functional kinase screening and database analysis, we identified ceritinib, an ALK inhibitor approved for the treatment of ALK-positive non-small cell lung cancer, as cytotoxic in MM cells. Notably, this effect is indepen-

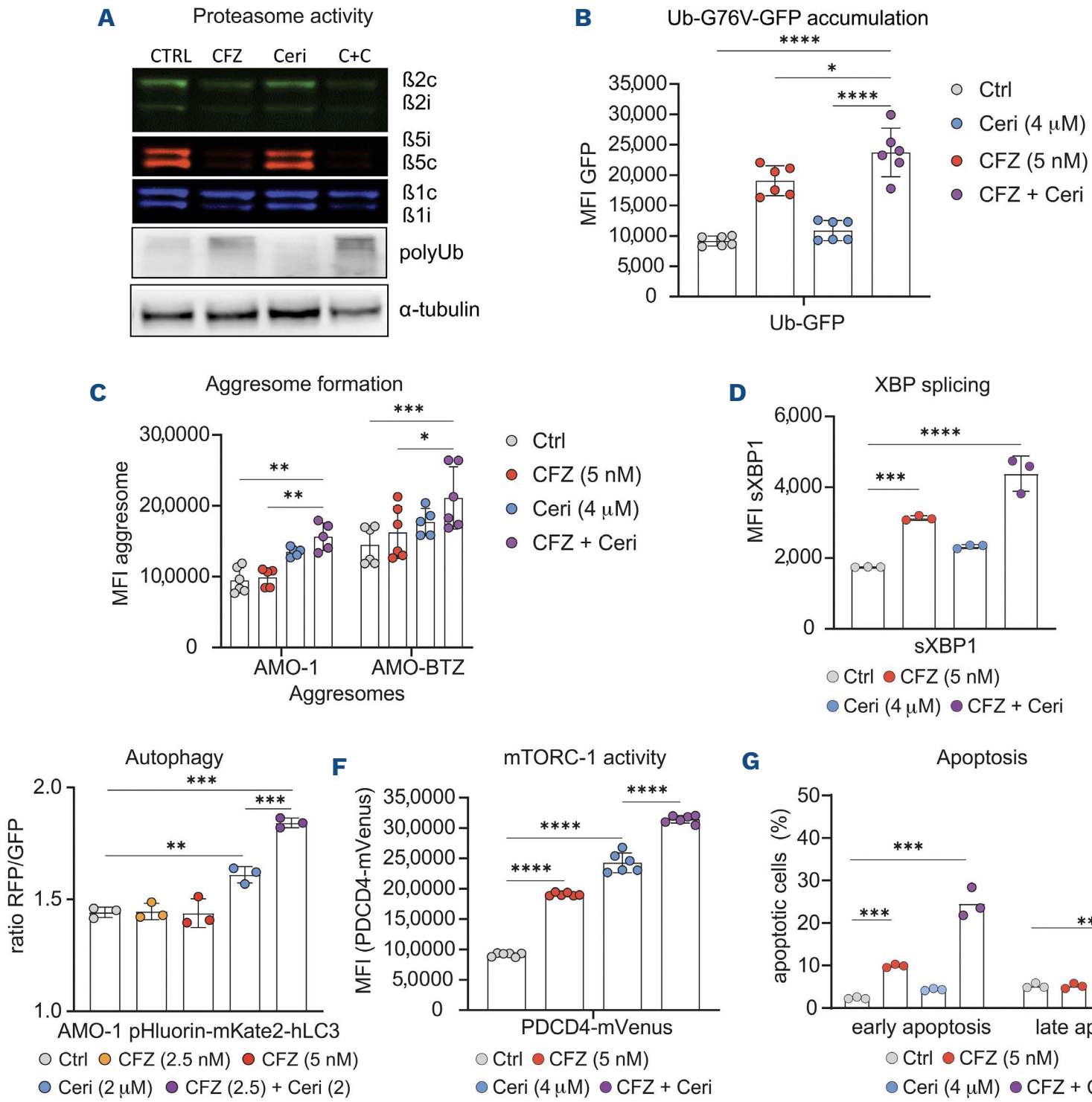

Figure 5. Ceritinib and carfilzomib synergistically induce polyubiquitinated protein accumulation, protein aggregation, and PDCD4 stabilization, triggering the unfolded protein response and autophagy, leading to terminal apoptosis. (A) Representative gel and Western blot analysis showing the activity of proteasome β1c/i, β2c/i, and β5c/i subunits, along with levels of polyubiquitinated proteins, following 8 hours of treatment with 5 nM carfilzomib, 4 μM ceritinib, or their combination. α-tubulin was used as a loading control. (B) Mean fluorescent intensity (MFI) of Ub-G76V-GFP reporter in AMO-1 cells after 12 hours of treatment with the indicated drugs. The data represent the mean ± standard deviation (SD) from six independent experiments. Statistical significance was assessed by one-way analysis of variance (ANOVA); **P*<0.05, *****P*<0.0001. (C) MFI of PROTEOSTAT® fluorescence, indicating protein aggregation in AMO-1 and proteasome inhibitor-adapted AMO-BTZ cells, after 20 hours of treatment with 5 nM carfilzomib, 4 μM ceritinib, or their combination. The data represent the mean ± SD from at least five independent experiments. Statistical analysis was assessed by one-way ANOVA; **P*<0.05, ***P*<0.01, ****P*<0.001. (D) MFI of spliced XBP1 in AMO-1 cells after 8 hours of treatment. The data represent the mean ± SD from three independent experiments. Statistical significance was determined by one-way ANOVA; ****P*<0.001. (E) Ratio of RFP (pH-unstable) to GFP (pH-stable) fluorescence in an endosomal pH sensor assay in AMO-1 cells treated for 8 hours with the indicated drugs. The data represent the mean ± SD from three independent experiments. Statistical significance was assessed by one-way ANOVA: **P*<0.05, ***P*<0.01, ****P*<0.001. (F) MFI of PDCD4-mVenus reporter in AMO-1 cells after 12 hours of treatment. The data represent the mean ± SD from three independent experiments in duplicate. Statistical significance was assessed by one-way ANOVA: *****P*<0.0001. (G) Quantification of early (annexin V^+/$FITC^-$) and late (annexin V^+/$FITC^+$) apoptotic cells in AMO-1 after 24 hours of treatment. The data represent the mean ± SD from three independent experiments. Statistical significance was assessed by two-way ANOVA; ****P*<0.001. PolyUb: polyubiquitinated proteins; Ctrl: control; CFZ: carfilzomib; Ceri: ceritinib; C+C: combination of ceritinib and carfilzomib; MFI: median fluorescence intensity; GFP: green fluorescence protein; RFP: red fluorescence protein; sXBP1: spliced X-box binding protein 1; PDCD4: programmed cell death 4.

dent of ALK, which is not expressed in MM, and instead results from ceritinib's inhibition of IGF-1R and INSR, both of which are expressed in MM and further upregulated in relapsed/refractory MM. Ceritinib demonstrated selective cytotoxicity across a panel of MM cell lines and primary MM patients' samples, while showing minimal activity in other hematologic malignancies.[20]

By integrating functional genome-wide screening, RNA sequencing, and *in vitro* assays, we demonstrate that ceritinib inhibits the IGF-1R/INSR axis, leading to suppression of PI3K/Akt/mTORC1 signaling, a pathway critical for supporting the high protein synthesis demands of MM cells, particularly the production of HSP such as HSP70. In parallel, INSR and IGF-1R signaling drive metabolic activity and glucose uptake, fueling nucleotide biosynthesis essential for replication, transcription, and translation. While MM cell dependence

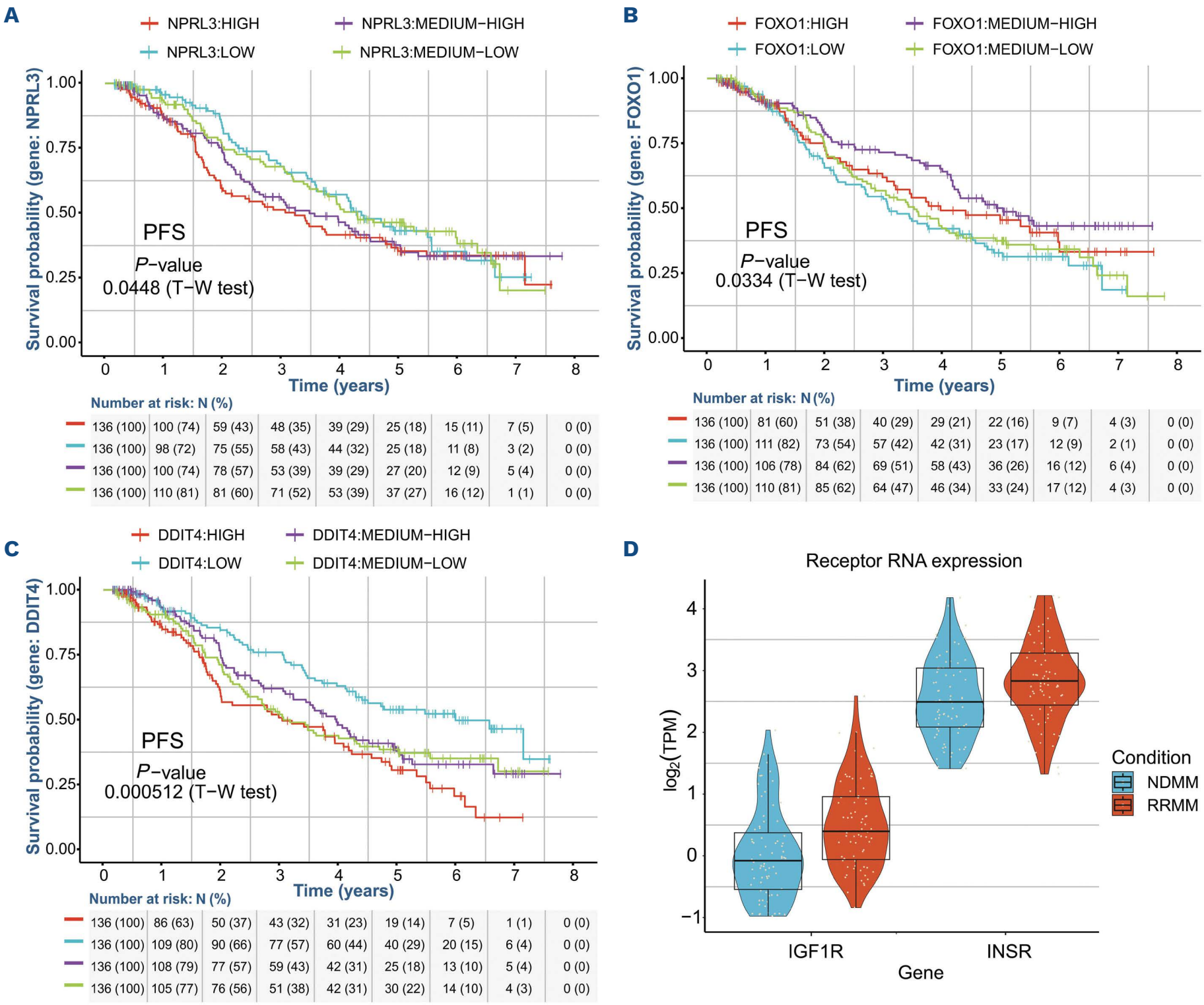

Figure 6. Prognostic relevance of selected genes and receptor expression in multiple myeloma patients. (A) Impact of *NPRL3* expression on progression-free survival (PFS) in multiple myeloma (MM) patients from the CoMMpass dataset. *P* values <0.05 were considered statistically significant. Statistical significance was assessed by a Tarone-Ware (T-W) test. (B) Impact of *FOXO1* expression on PFS in MM patients from the CoMMpass dataset. *P* values <0.05 were considered statistically significant. Statistical significance was assessed by a T-W test. (C) Impact of *DDIT4* expression on PFS in MM patients from the CoMMpass dataset. *P* values <0.05 were considered statistically significant. Statistical significance was assessed by a T-W test. (D) Expression levels of *IGF1R* and *INSR* in newly diagnosed MM patients (CoMMpass dataset) and in a cohort of patients with relapsed/refractory MM from Würzburg University Hospital. *NPRL3*: NPR3 like, GATOR1 complex subunit; *FOXO1*: forkhead box O1; *DDIT4*: DNA damage inducible transcript 4; TPM: transcripts per million; *IGF1R*: insulin like growth factor 1 receptor; *INSR*: insulin receptor; NDMM: newly diagnosed multiple myeloma; RRMM: relapsed/refractory multiple myeloma.

on Akt/mTORC signaling is well established,[28,32,33] our data highlight a specific reliance on IGF-1R/INSR to maintain elevated HSP70 levels, aligning with previous reports of insulin-mediated regulation of HSP and factors.[34]

FOXO-1 and cell-intrinsic negative regulators of mTORC1, including NPRL2, NPRL3, and DDIT4, play a crucial role in the cytotoxicity of ceritinib in MM cells. Activated FOXO-1 inhibits mTORC1 through both Tuberous Sclerosis Complex (TSC)2-dependent and independent mechanisms.[25] DDIT4 inhibits mTORC1 activity via the TSC1/TSC2 complex, a critical regulator of mTORC1 that is triggered by growth factors, such as insulin.[35] In contrast, NPRL2 and NPRL3 form the GATOR1 complex, which is a pivotal regulator of the pathway that signals amino acid sufficiency to mTORC1 and inhibits mTORC1 activity during intracellular amino acid starvation.[36] Given these insights, the highly active mTORC1 complex appears to be crucial for the cytotoxicity of ceritinib. It also significantly impacts the outcome of MM patients. High FOXO-1 levels are associated with a better prognosis, while elevated NPRL3 and DDIT4 levels have a negative impact on MM patients' survival. Consistently, high FOXO-1 levels have been associated with better overall survival of MM patients,[28] while low FOXO-1 levels correlate with poor prognosis in patients with myelodysplastic syndrome.[37] Similarly, DDIT4 is associated with a poor prognosis in solid tumors,[38,39] as well as in hematologic cancers, such as acute myeloid leukemia[40] and MM.[41]

Our data demonstrate that ceritinib can be combined with carfilzomib to overcome PI resistance in multiple MM cell lines *in vitro*, in primary samples from patients with relapsed/refractory MM or PCL, and in an orthotopic PI-resistant *in vivo* model. This is particularly important in the context of bone marrow microenvironment-driven MM resistance, which is mediated by the interaction between MM cells and surrounding mesenchymal stem cells, and which depends on high PI3K/Akt/mTOR signaling.[42] Consistently, selective Akt inhibition enhances cytotoxicity of proteasome inhibition.[43] The strong synergy between ceritinib and carfilzomib reflects dual disruption of protein homeostasis, specifically protein folding and degradation. Carfilzomib induces a pro-survival induction of HSP and chaperones actively compensating for the inability to degrade proteins.[3] In line with this, selective inhibition of HSP70 sensitizes multiple cell lines to carfilzomib.[3] Since ceritinib inhibits HSP70 protein induction, the combination treatment results in the accumulation of protein aggregates, ER stress, and autophagy in MM cells, collectively promoting apoptosis. Additionally, mTORC1 and the ubiquitin-proteasome system are tightly linked through amino acid and nutrient sensing. mTORC1 inhibition activates both the ubiquitin-proteasome system and autophagy, promoting amino acid recycling and slowing cell growth,[44,45] while proteasome inhibition depletes amino acids, triggering cell death if not replenished.[46] This dependency on protein recycling has been exploited therapeutically.[47] Previous preclinical data with novel inhibitors of the PI3K/Akt/mTORC1 pathway (copanlisib, montelukast) or depletion of amino acids in combination with carfilzomib reported synergistic drug combinations in PI-sensitive and PI-resistant models[48-50] supporting our findings of dual targeting of these pathways to achieve an anti-MM effect.

While these data provide compelling preclinical evidence for the combination of ceritinib and carfilzomib, certain limitations should be acknowledged. The use of PI-adapted cell lines generated *in vitro* may not fully represent the complexity and heterogeneity of clinical resistance. Furthermore, xenograft studies based on these lines do not reproduce the full immune and stromal interactions of the human bone marrow microenvironment, underscoring the need for validation in patient-derived models.

In summary, these findings highlight a potential off-the-shelf combination therapy that could overcome therapy resistance in MM and provide a strong rationale for further preclinical and clinical testing in the setting of relapsed/refractory MM.

Disclosures

No conflicts of interest to disclose.

Contributions

AB designed and performed the majority of the in vitro and in vivo experiments and prepared the manuscript and figures. MK, KM, JV, LS and MML contributed to the in vitro and in vivo experiments. TJ performed measurements on Incucyte. MT and CH performed the RNA-sequencing of the cohort of patients from Würzburg. TT and MB analyzed the patients' datasets. KMK and LR provided samples from relapsed/refractory MM patients. APAJ and MvdS conducted the analysis of the ChEMBL database. CD secured funding and provided critical review of the data. LB conceptualized the study, secured funding, and wrote the manuscript. All authors reviewed and edited the manuscript.

Funding

The work was supported by Wilhelm-Sander Stiftung (2021.077.1), Cantonal Hospital St. Gallen Research Committee internal grant N 20/41 and by the project National Institute for Cancer Research (Program EXCELES, ID Project N. LX22NPO5102) - funded by the European Union – Next Generation EU.

Data-sharing statement

Raw data from RNA-sequencing and genome-wide CRISPR Cas9 screening (DNA-sequencing) is available at the BioStudies database from the European Molecular Biology Laboratory - European Bioinformatics Institute EMBL-EBI) website, https://www.ebi.ac.uk/biostudies/ under accession numbers E-MTAB-15466 and E-MTAB-15465. All other data are available upon request to the corresponding author.

References

1. Gandolfi S, Laubach JP, Hideshima T, et al. The proteasome and proteasome inhibitors in multiple myeloma. Cancer Metastasis Rev. 2017;36(4):561-584.
2. Mitsiades N, Mitsiades CS, Poulaki V, et al. Molecular sequelae of proteasome inhibition in human multiple myeloma cells. Proc Natl Acad Sci U S A. 2002;99(22):14374-14379.
3. Oron M, Grochowski M, Jaiswar A, et al. The molecular network of the proteasome machinery inhibition response is orchestrated by HSP70, revealing vulnerabilities in cancer cells. Cell Rep. 2022;40(13):111428.
4. Huang L, Wang Y, Bai J, et al. Blockade of HSP70 by VER-155008 synergistically enhances bortezomib-induced cytotoxicity in multiple myeloma. Cell Stress Chaperones. 2020;25(2):357-367.
5. Ishii T, Seike T, Nakashima T, et al. Anti-tumor activity against multiple myeloma by combination of KW-2478, an Hsp90 inhibitor, with bortezomib. Blood Cancer J. 2012;2(4):e68.
6. Ferguson ID, Lin YT, Lam C, et al. Allosteric HSP70 inhibitors perturb mitochondrial proteostasis and overcome proteasome inhibitor resistance in multiple myeloma. Cell Chem Biol. 2022;29(8):1288-1302.
7. Seggewiss-Bernhardt R, Bargou RC, Goh YT, et al. Phase 1/1B trial of the heat shock protein 90 inhibitor NVP-AUY922 as monotherapy or in combination with bortezomib in patients with relapsed or refractory multiple myeloma. Cancer. 2015;121(13):2185-2192.
8. Georgii-Hemming P, Wiklund HJ, Ljunggren O, Nilsson K. Insulin-like growth factor I is a growth and survival factor in human multiple myeloma cell lines. Blood. 1996;88(6):2250-2258.
9. Sprynski AC, Hose D, Caillot L, et al. The role of IGF-1 as a major growth factor for myeloma cell lines and the prognostic relevance of the expression of its receptor. Blood. 2009;113(19):4614-4626.
10. Sprynski AC, Hose D, Kassambara A, et al. Insulin is a potent myeloma cell growth factor through insulin/IGF-1 hybrid receptor activation. Leukemia. 2010;24(11):1940-1950.
11. De Meyts P, Whittaker J. Structural biology of insulin and IGF1 receptors: implications for drug design. Nat Rev Drug Discov. 2002;1(10):769-783.
12. Cai W, Sakaguchi M, Kleinridders A, et al. Domain-dependent effects of insulin and IGF-1 receptors on signalling and gene expression. Nat Commun. 2017;8:14892.
13. Mitsiades CS, Mitsiades NS, McMullan CJ, et al. Inhibition of the insulin-like growth factor receptor-1 tyrosine kinase activity as a therapeutic strategy for multiple myeloma, other hematologic malignancies, and solid tumors. Cancer Cell. 2004;5(3):221-230.
14. Kuhn DJ, Berkova Z, Jones RJ, et al. Targeting the insulin-like growth factor-1 receptor to overcome bortezomib resistance in preclinical models of multiple myeloma. Blood. 2012;120(16):3260-3270.
15. Tanaka Y, Okabe S, Tauchi T, Ito Y, Ohyashiki K. Targeting insulin-like growth factor in multiple myeloma: novel strategies in the treatment of proteasome inhibitor resistant cells. Blood. 2018;132(Supplement 1):5155.
16. Shaw AT, Kim DW, Mehra R, et al. Ceritinib in ALK-rearranged non-small-cell lung cancer. N Engl J Med. 2014;370(13):1189-1197.
17. van Erp AEM, Hillebrandt-Roeffen MHS, van Houdt L, Fleuren EDG, van der Graaf WTA, Versleijen-Jonkers YMH. Targeting anaplastic lymphoma kinase (ALK) in rhabdomyosarcoma (RMS) with the second-generation ALK inhibitor ceritinib. Target Oncol. 2017;12(6):815-826.
18. Vewinger N, Huprich S, Seidmann L, et al. IGF1R is a potential new therapeutic target for HGNET-BCOR brain tumor patients. Int J Mol Sci. 2019;20(12):3027.
19. Russo A, Paret C, Alt F, et al. Ceritinib-induced regression of an insulin-like growth factor-driven neuroepithelial brain tumor. Int J Mol Sci. 2019;20(17):4267.
20. Bonolo de Campos C, Meurice N, Petit JL, et al. "Direct to Drug" screening as a precision medicine tool in multiple myeloma. Blood Cancer J. 2020;10(5):54.
21. Besse A, Besse L, Kraus M, et al. Proteasome inhibition in multiple myeloma: head-to-head comparison of currently available proteasome inhibitors. Cell Chem Biol. 2019;26(3):340-351.
22. Besse L, Besse A, Stolze SC, et al. Treatment with HIV-protease inhibitor nelfinavir identifies membrane lipid composition and fluidity as a therapeutic target in advanced multiple myeloma. Cancer Res. 2021;81(17):4581-4593.
23. Li W, Koster J, Xu H, et al. Quality control, modeling, and visualization of CRISPR screens with MAGeCK-VISPR. Genome Biol. 2015;16:281.
24. Soriano GP, Besse L, Li N, et al. Proteasome inhibitor-adapted myeloma cells are largely independent from proteasome activity and show complex proteomic changes, in particular in redox and energy metabolism. Leukemia. 2016;30(11):2198-2207.
25. Chen CC, Jeon SM, Bhaskar PT, et al. FoxOs inhibit mTORC1 and activate Akt by inducing the expression of Sestrin3 and Rictor. Dev Cell. 2010;18(4):592-604.
26. Geffken SJ, Moon S, Smith CO, et al. Insulin and IGF-1 elicit robust transcriptional regulation to modulate autophagy in astrocytes. Mol Metab. 2022;66:101647.
27. Yee LD, Mortimer JE, Natarajan R, Dietze EC, Seewaldt VL. Metabolic health, insulin, and breast cancer: why oncologists should care about insulin. Front Endocrinol (Lausanne). 2020;11:58.
28. Bloedjes TA, de Wilde G, Maas C, et al. AKT signaling restrains tumor suppressive functions of FOXO transcription factors and GSK3 kinase in multiple myeloma. Blood Adv. 2020;4(17):4151-4164.
29. Moustafa-Kamal M, Kucharski TJ, El-Assaad W, et al. The mTORC1/S6K/PDCD4/eIF4A axis determines outcome of mitotic arrest. Cell Rep. 2020;33(1):108230.
30. Paroha R, Wang J, Lee S. PDCD4 as a marker of mTOR pathway activation and therapeutic target in mycobacterial infections. Microbiol Spectr. 2024;12(8):e0006224.
31. Bieghs L, Johnsen HE, Maes K, et al. The insulin-like growth factor system in multiple myeloma: diagnostic and therapeutic potential. Oncotarget. 2016;7(30):48732-48752.
32. Hsu J, Shi Y, Krajewski S, et al. The AKT kinase is activated in multiple myeloma tumor cells. Blood. 2001;98(9):2853-2855.
33. Peterson TR, Laplante M, Thoreen CC, et al. DEPTOR is an mTOR inhibitor frequently overexpressed in multiple myeloma cells and required for their survival. Cell. 2009;137(5):873-886.
34. Ting LP, Tu CL, Chou CK. Insulin-induced expression of human heat-shock protein gene hsp70. J Biol Chem. 1989;264(6):3404-3408.
35. Tirado-Hurtado I, Fajardo W, Pinto JA. DNA damage inducible transcript 4 gene: the switch of the metabolism as potential target in cancer. Front Oncol. 2018;8:106.

36. Bar-Peled L, Chantranupong L, Cherniack AD, et al. A tumor suppressor complex with GAP activity for the Rag GTPases that signal amino acid sufficiency to mTORC1. Science. 2013;340(6136):1100-1106.
37. Zhang Z, Huang N, Xv F, et al. Decreased FOXO1 expression is correlated with poor prognosis in myelodysplastic syndromes. Curr Oncol. 2022;29(10):6933-6946.
38. Song L, Chen Z, Zhang M, et al. DDIT4 overexpression associates with poor prognosis in lung adenocarcinoma. J Cancer. 2021;12(21):6422-6428.
39. Chen X, Li Z, Liang M et, al. Identification of DDIT4 as a potential prognostic marker associated with chemotherapeutic and immunotherapeutic response in triple-negative breast cancer. World J Surg Oncol. 2023;21(1):194.
40. Cheng Z, Dai Y, Pang Y, et al. Up-regulation of DDIT4 predicts poor prognosis in acute myeloid leukaemia. J Cell Mol Med. 2020;24(1):1067-1075.
41. Yu Z, Qiu B, Li L, Xu J, Zhou H, Niu T. An emerging prognosis prediction model for multiple myeloma: Hypoxia-immune related microenvironmental gene signature. Front Oncol. 2022;12:992387.
42. Heinemann L, Mollers KM, Ahmed HMM, et al. Inhibiting PI3K-AKT-mTOR signaling in multiple myeloma-associated mesenchymal stem cells impedes the proliferation of multiple myeloma cells. Front Oncol. 2022;12:874325.
43. Mimura N, Hideshima T, Shimomura T, et al. Selective and potent Akt inhibition triggers anti-myeloma activities and enhances fatal endoplasmic reticulum stress induced by proteasome inhibition. Cancer Res. 2014;74(16):4458-4469.
44. Zhao J, Zhai B, Gygi SP, Goldberg AL. mTOR inhibition activates overall protein degradation by the ubiquitin proteasome system as well as by autophagy. Proc Natl Acad Sci U S A. 2015;112(52):15790-15797.
45. Zhao J, Garcia GA, Goldberg AL. Control of proteasomal proteolysis by mTOR. Nature. 2016;529(7586):E1-2.
46. Suraweera A, Munch C, Hanssum A, Bertolotti A. Failure of amino acid homeostasis causes cell death following proteasome inhibition. Mol Cell. 2012;48(2):242-253.
47. Saavedra-Garcia P, Roman-Trufero M, Al-Sadah HA, et al. Systems level profiling of chemotherapy-induced stress resolution in cancer cells reveals druggable trade-offs. Proc Natl Acad Sci U S A. 2021;118(17):e2018229118.
48. Okabe S, Tanaka Y, Tauchi T, Ohyashiki K. Copanlisib, a novel phosphoinositide 3-kinase inhibitor, combined with carfilzomib inhibits multiple myeloma cell proliferation. Ann Hematol. 2019;98(3):723-733.
49. Tong J, Yu Q, Xu W, et al. Montelukast enhances cytocidal effects of carfilzomib in multiple myeloma by inhibiting mTOR pathway. Cancer Biol Ther. 2019;20(3):381-390.
50. Soncini D, Minetto P, Martinuzzi C, et al. Amino acid depletion triggered by L-asparaginase sensitizes MM cells to carfilzomib by inducing mitochondria ROS-mediated cell death. Blood Adv. 2020;4(18):4312-4326.